Connecting the dots

Delineating the regulation of H3K79 methylation by Dot1

Vlaming, H.

Publication date
2017

Document Version
Other version

License
Other

4

Flexibility in crosstalk between H2B ubiquitination and H3 methylation *in vivo*

Hanneke Vlaming[1], Tibor van Welsem[1], Erik L. de Graaf[2], David Ontoso[3] A.F. Maarten Altelaar[2], Pedro A. San-Segundo[3], Albert J.R. Heck[2], Fred van Leeuwen[1]

[1] Division of Gene Regulation, Netherlands Cancer Institute, Amsterdam, The Netherlands
[2] Biomolecular Mass Spectrometry and Proteomics Group, The Netherlands Proteomics Centre, Utrecht University, Utrecht, The Netherlands

[3] Instituto de Biologa Funcional y Genmica, CSIC/University of Salamanca, Salamanca, Spain

Published in:
EMBO Reports, 2014.

4.1 Abstract

Histone H2B ubiquitination is a dynamic modification that promotes methylation of histone H3K79 and H3K4. This crosstalk is important for DNA damage response and has been implicated in cancer. In engineered yeast strains, ubiquitins tethered to every nucleosome promoted H3K79 and H3K4 methylation from a proximal as well as a more distal site, but only if in a correct orientation. This plasticity indicates that the exact location of the attachment site, the native ubiquitin-lysine linkage and ubiquitination cycles are not critical for trans-histone crosstalk *in vivo*. The flexibility in crosstalk indicates that other ubiquitination events may also promote H3 methylation.

Keywords

Chromatin; crosstalk; Dot1; histone ubiquitination; Set1

4.2 Introduction

The DNA in the nucleus is wrapped around octamers of histone proteins. Histones can be modified and these post-translational modifications (PTMs) regulate most processes that occur at the DNA. In turn, histone PTMs are regulated by signaling events in the cell, such as other histone PTMs. This crosstalk can occur between PTMs on the same histone, but also between histones.

An evolutionary-conserved trans-histone crosstalk is that between ubiquitin on the C terminus of histone H2B and methylation of histone H3 on lysine 79 (H3K79) and lysine 4 (H3K4) (Figure 4.1A). In yeast, H2B is ubiquitinated on lysine 123 (H2BK123) by the Rad6/Bre1 complex, which enhances the overall activity of Dot1 (Figure 4.1B) and activates the Set1 complex (COMPASS) (Nakanishi et al., 2009, and references therein). Whereas H2Bub is a transient mark, H3K4 and especially H3K79 methylation are more stable and will remain after H2Bub has been removed (Gardner et al., 2005; Schulze et al., 2011). In mammalian cells, ubiquitination of H2B by RNF20/40 promotes H3K79 methylation by *DOT1*L, and H3K4 methylation by several Set1/MLL complexes (Kim et al., 2013; Zhu et al., 2005b). As proliferation in MLL-rearranged leukemias depends on RNF20, DOT1L and MLL1, this trans-histone crosstalk may have a role in cancer (Jo et al., 2011; Thiel et al., 2010; Wang et al., 2013).

In general, despite intensive studies, how monoubiquitin acts as a signal often remains unknown (Husnjak and Dikic, 2012). For the role of ubiquitinated H2B (H2Bub) in promoting Dot1 activity, two non-exclusive models have been suggested: a wedge model and a bridge model (reviewed in Braun and Madhani, 2012; Chandrasekharan et al., 2010). The wedge model, in which the ubiquitin moiety disrupts chromatin structure and enables Dot1 to access the nucleosome core surface, is supported by *in vitro* experiments that showed that ubiquitin on H2B disrupts chromatin compaction (Fierz et al., 2011). However, since the crosstalk can occur on mononucleosomes (Chatterjee et al., 2010; McGinty et al., 2008), the opening of the chromatin cannot be the only mechanism behind the crosstalk. Moreover, *in vivo*, H2Bub may actually lead to chromatin compaction (Batta et al., 2011; Chandrasekharan et al., 2009; Fleming et al., 2008). In the bridge model, ubiquitin functions as a bridge to recruit or activate Dot1. However, Dot1 has a similar affinity for both ubiquitinated and unmodified nucleosomes (McGinty et al., 2008) and the only putative ubiquitin-binding domain in Dot1 (Oh et al., 2010) is not required for the crosstalk (De Vos et al., 2011).

Although the molecular mechanisms remain elusive, *in vitro* studies have revealed that there is some plasticity in this remarkable histone crosstalk. Ubiquitin confers crosstalk when linked to various residues in the vicinity of H2BK123, and the ubiquitin-like modifier Nedd8 can stimulate Dot1 as strongly as ubiquitin itself(Chatterjee et al., 2010). Whether similar rules apply to the crosstalk *in vivo* is an important next question that remains to be addressed. However, studying the function of one specific ubiquitination event on one particular target *in vivo* is challenging (Williamson et al., 2013). We took advantage of the

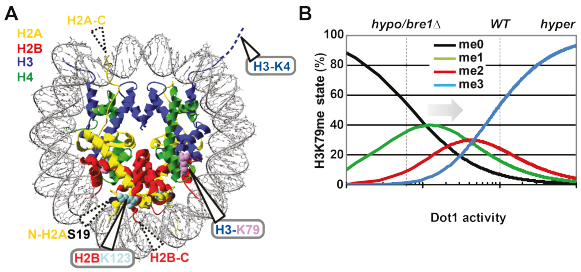

Figure 4.1: Location of H2B ubiquitin and its role in H3K79 methylation. A) Nucleosome core particle in which H2BK123, H3K79 and H3K4 are indicated as well as the sites of linear ubiquitin attachment described below. Most of the unstructured N- and C-terminal histone tails are absent from this structure; the histone ends fused to ubiquitin (see below) are indicated with dashed triangles. **B)** Dependence of H3K79me levels on Dot1 activity, modified from (De Vos et al., 2011). Dashed lines indicate approximate H3K79me levels in WT or *bre1*Δ cells. Arrow indicates the direction of the changes expected upon positive histone crosstalk.

possibility to engineer complex histone mutants in budding yeast, to learn which molecular features of ubiquitinated H2B are important for the trans-histone crosstalk to H3 methylation *in vivo*. Our experiments using ubiquitins tethered to the nucleosome reveal that the crosstalk from ubiquitination to methylation has a high degree of plasticity *in vivo*. Our study leads to new insights about the molecular determinants and provides support for a new model for the crosstalk towards H3K79 methylation.

4.3 Results

Ubiquitin tethered to the N terminus of H2A confers crosstalk to H3K79 methylation

To specifically determine the features of H2Bub that promote histone methylation at H3K79 and H3K4 *in vivo*, we designed yeast strains in which the endogenous H2Bub pathway was eliminated by deletion of *BRE1* and in which a ubiquitin moiety was specifically re-introduced on the nucleosome. We used a plasmid shuffle assay to create strains in which an engineered H2A gene was the only source of H2A protein (Supplementary Figure 4.1A and B). Ubiquitin (ub) was tethered via a short HA tag to H2A at S1 or at S19, in close proximity to H2BK123 (Figure 4.1A). The terminal glycine of ub was removed to prevent ub-H2A cleavage (Supplementary Figure 4.1D). Strains expressing HA-S1-H2A, ubHA-S1-H2A or ubHA-S19-H2A were viable (Supplementary Figure 4.1B and D), suggesting that these fusions showed no gross defects in histone transport, assembly, and chromatin packaging. The HA-S19-H2A-expressing *bre1*Δ strain was not viable and was eliminated from further analyses, see Supplementary Figure 4.1B. Immunoblot analysis confirmed that the H2A fusion proteins were

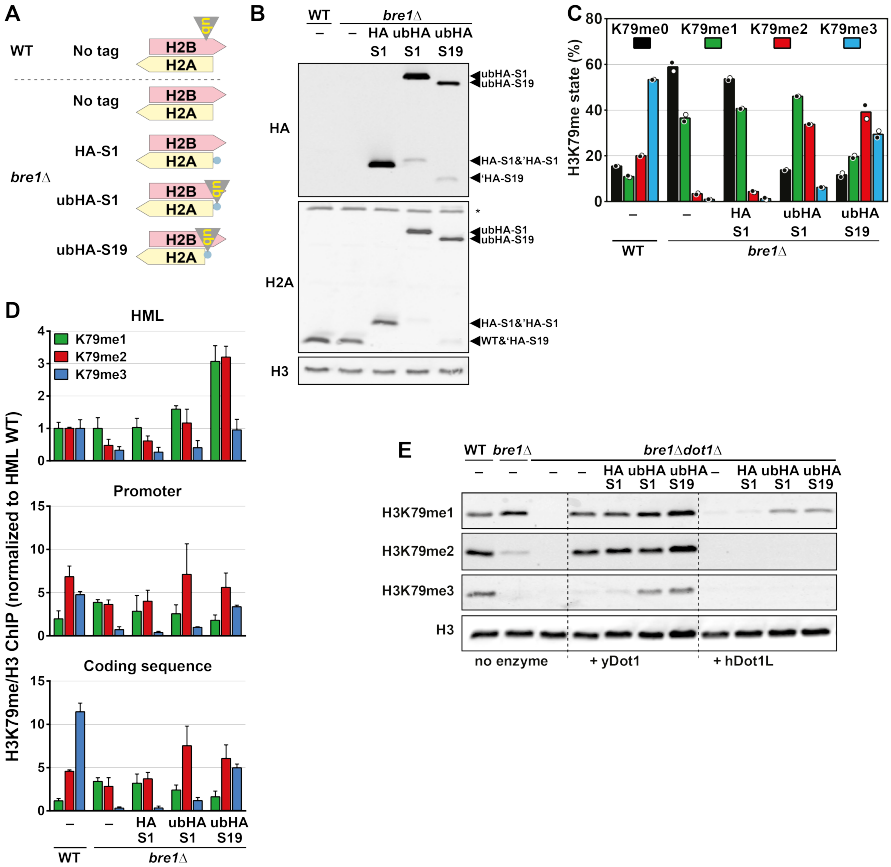

Figure 4.2: Ubiquitin on the H2A N terminus promotes H3K79 methylation *in vivo* and *in vitro*. **A)** Cartoon of H2A/H2B in the used strains. **B)** Immunoblot analysis shows tagged H2A and the absence of endogenous wild-type H2A. Asterisk indicates non-specific signal. 'HA indicates ubHA-H2A proteins that lost the ub moiety due to the activity of ubiquitin-specific proteases. **C)** MS analysis of H3K79 methylation levels in strains shown in panel A and B (mean and individual data points of two biological replicates). See also Supplementary Figure 4.1F. **D)** ChIP-qPCR data of the different methylation states at three loci. Values for each methyl antibody were normalized to H3, after which all values were normalized per methyl antibody to wildtype at the *HML* locus. Primer sets against *HML*, the promoter of the *GAL1* gene and the coding sequence of *SPA2* were used. Mean ± SD of three biological replicates is shown. **E)** Immunoblot analysis of the *in vitro* methyltransferase activity of purified 10xHis-tagged yeast or human Dot1 protein towards chromatin templates isolated from yeast strains lacking Dot1 and Bre1 and expressing wild-type H2A or N-terminal fusions of H2A. See also Supplementary Figure 4.1H.

expressed, that no wild-type H2A was present, and that the majority of the fusions were full-length (Figure 4.2B). ChIP-qPCR experiments confirmed that tagged H2A was incorporated into chromatin (Supplementary Figure 4.1E).

Multiple methylation by Dot1 occurs by a distributive mechanism, which leads to a characteristic shift in the relative abundance of the H3K79 methyla-

tion states when the activity of Dot1 increases or decreases (Figure 4.1B) (De Vos et al., 2011; Frederiks et al., 2008). The ubiquitin moiety at H2AS19, close to the native position of ubiquitination, caused a shift from H3K79me0/me1 to H3K79me2/me3, while Dot1 expression was not increased (Figure 4.2C, Supplementary Figure 4.1F). Unexpectedly, the more distal ubiquitin at S1 of H2A was also able to promote H3K79 methylation, albeit with a somewhat lower efficiency (Figure 4.2C). This did not require the formation of ubiquitin branches, since K0 mutants of ubiquitin could still promote H3K79 methylation (Supplementary Figure 4.1G). H3K79 methylation is not distributed uniformly across the genome, but is very low in heterochromatin, intermediate in intergenic regions, and high in coding sequences (see Figure 4.2D) (Schulze et al., 2009). In a *bre1*Δ strain a shift to lower methylation states was observed at all loci (in line with the distributive mechanism, see Figure 4.1B). Tethered ubiquitins increased methylation at all tested loci. The H3K79 methylation in strains expressing histone-ubiquitin fusions was more evenly distributed than in wild-type cells with native H2Bub (Figure 4.2D), confirming that this crosstalk contributes to the establishment of the H3K79 methylation pattern. However, since the pattern was still partially maintained, additional mechanisms of regulation must exist, such as histone turnover (De Vos et al., 2011; Radman-Livaja et al., 2011) or protection of nucleosomes by binding of the Sir complex (Altaf et al., 2007).

Together, these findings show that a ubiquitin constitutively tethered to the N terminus of H2A by a linear fusion confers trans-histone crosstalk *in vivo*, throughout the genome. To eliminate indirect effects of the ub-H2A on H3K79 methylation, we performed *in vitro* methyltransferase assays using chromatin templates isolated from the engineered yeast strains. Ubiquitin tethered to the H2A N terminus promoted the activity of yeast Dot1 as well as human DOT1L *in vitro*, suggesting that it has a direct effect on Dot1 activity (Figure 4.2E and Supplementary Figure 4.1H).

Ubiquitin tethered to the C terminus of H2A or H2B confers modest crosstalk to H3K79 methylation

To find the limits of the observed plasticity, and thereby determine which features are important for the crosstalk, we created C-terminal fusions between histone H2A or H2B and ubiquitin (Supplementary Figure 4.2A). The C-terminal glycine of ub was changed to valine to avoid conjugation of the fusion protein to ubiquitination targets. Yeast strains expressing an H2A-ub or H2B-ub fusion protein were viable in the absence of untagged versions of the respective histones (Supplementary Figure 4.2B). Expression of the fusion proteins and the absence of untagged histone protein was confirmed by immunoblot analysis (Figure 4.3B).

In *bre1*Δ strains, lacking endogenous H2Bub, ubiquitins tethered to the C terminus of H2A or H2B led to more H3K79me1/me2 and less H3K79me0, while Dot1 expression was not increased (Figure 4.3C, Supplementary Figure 4.2C). However, they bypassed the lack of endogenous H2Bub only partially; ubiquitin tethered to the H2A or H2B C terminus was much less potent than ubiquitin

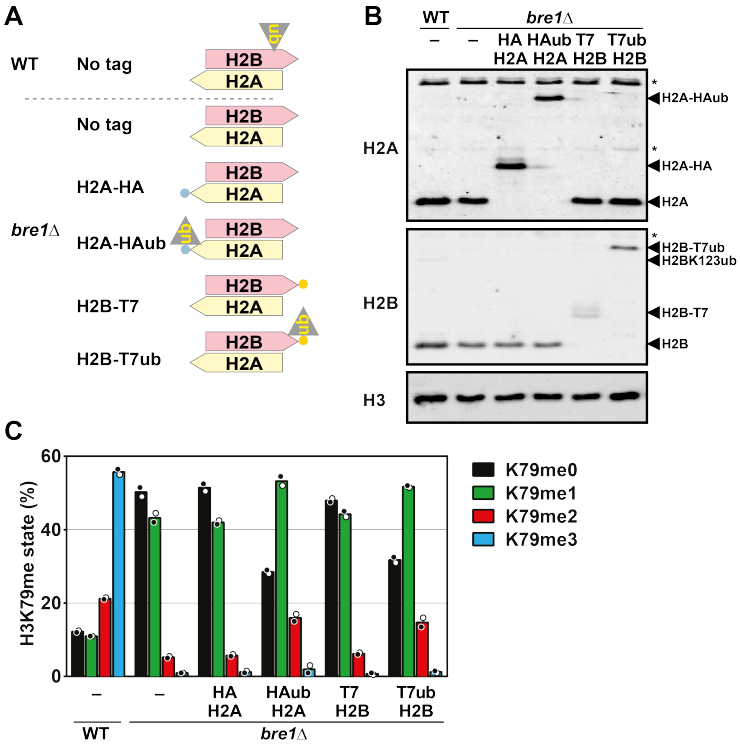

Figure 4.3: textbfUbiquitins tethered to the C terminus of H2A and H2B can modestly promote H3K79 methylation *in vivo*. A) Cartoon of H2A/H2B in the used strains. **B)** Immunoblot analysis of tagged and untagged histones. Asterisk indicates non-specific signal. **C)** MS analysis of H3K79 methylation levels in strains expressing H2A or H2B C-terminal ub fusions (mean and individual data points of two biological replicates). See also Supplementary Figure 4.2C.

tethered to the N terminus of H2A (see Figure 4.2C).

Ubiquitin crosstalk to H3K4 methylation

Having established that ubiquitin tethered to the nucleosome can take over the role of native H2Bub in promoting Dot1 activity, we asked whether they could also be used to gain insight into the crosstalk from H2Bub to H3K4 methylation. Using the engineered yeast strains we found that ub-H2A fully restored H3K4me1 and me2 and partially restored H3K4me3 in the absence of endogenous H2Bub (Figure 4.4A). H2A-ub did not promote H3K4 methylation and H2B-ub had a modest effect (Figure 4.4A). Taken together, the findings indicate that also the crosstalk to H3K4 methylation is plastic and that Dot1 and Set1 require overlapping but also distinct structural features of chromatin containing H2Bub (Supplementary Table 4.1).

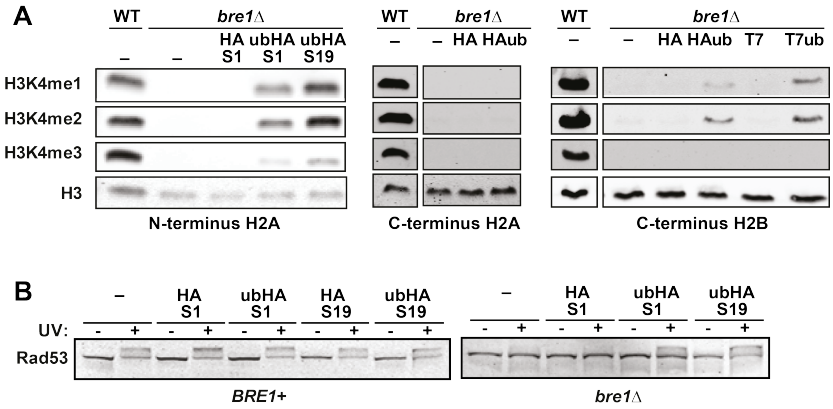

Figure 4.4: Tethered ubiquitins can promote H3K4 methylation and DNA damage checkpoint activation. A) Immunoblot analysis of H3K4 methylation in strains expressing various histone-ubiquitin fusions. **B)** Immunoblot analysis of activation of the central DNA damage checkpoint kinase Rad53 upon exposure of yeast cells arrested in G1/S to 100 J m^{-2} UV irradiation. Rad53 is activated by phosphorylation, which leads to a mobility shift.

Tethered ubiquitins substitute for native H2B ubiquitination in the DNA damage response

H2B ubiquitination and H3K79 methylation are required for a timely induction of the DNA damage response (Jackson and Durocher, 2013a). However, whether dynamic changes in H2Bub or histone methylation are required is unknown. Two general models have been proposed: i) due to global H2Bub and H3K79me, checkpoint proteins are at the DNA and can be phosphorylated upon DNA damage, ii) a local increase in H2Bub and H3K79me at the site of lesion recruits and/or activates checkpoint proteins (Giannattasio et al., 2005; Moyal et al., 2011; Shiloh et al., 2011). We investigated this problem, using phosphorylation of the central kinase Rad53 as the readout of checkpoint activation after UV irradiation of G1-arrested cells. Whereas *bre1*Δ cells poorly phosphorylated Rad53 upon UV irradiation (Figure 4.4B), tethered ubiquitins restored Rad53 phosphorylation in *bre1*Δ cells (visible as an upward shift of the protein, Figure 4.4B and Supplementary Figure 4.3A). Since the constitutive ubiquitin moieties on each nucleosome are sufficient for checkpoint activation after UV, we conclude that a local accumulation of H2Bub specifically at the site of damage is not required. Instead, the data suggest a role of global chromatin modification in modulating the DNA damage checkpoint. In addition, since the ubiquitin tethers are static, our results demonstrate that cycles of ubiquitination and deubiquitination are not required for DNA damage checkpoint activation.

4.4 Discussion

The crosstalk between H2B ubiquitination and H3K4 and H3K79 methylation is evolutionary conserved from yeast to metazoans. Since many other chromatin proteins are also subject to ubiquitination, an important question is which molecular features of ubiquitinated H2B are important for the trans-histone crosstalk *in vivo*. We have shown that various tethered ubiquitins, expressed as linear histone-ubiquitin fusions, can substitute for native H2BK123ub in the crosstalk to H3K79 and H3K4 methylation. This reveals an unexpected plasticity in the crosstalk *in vivo*.

The extent of the plasticity in the crosstalk *in vivo* is remarkable. Previously, *in vitro* experiments already revealed some plasticity in the site of ubiquitin attachment (Chatterjee et al., 2010; Wu et al., 2013b). However, the *in vivo* plasticity of the crosstalk observed here goes beyond what has so far been observed *in vitro*. This allows us to draw several conclusions about the features of H2Bub that are important for crosstalk to H3 methylation.

First, the precise location of ubiquitin attachment to the nucleosome core surface is not critical for nucleosome crosstalk since H3K79 and H3K4 methylation were enhanced by ubiquitin tethered to various positions on the nucleosome. This is in line with the finding that ubiquitination of H2BK34 by MSL2 stimulates H3K79 and H3K4 methylation in human cell lines and *in vitro* (Wu et al., 2011b). In contrast to the previous finding that a short linker between ubiquitin and H2B decreases the crosstalk considerably *in vitro* (Chatterjee et al., 2010), ubiquitin tethered to H2AS1 was approximately as effective as ubiquitin on H2AS19. Note that the ubiquitin tethered to H2AS1 is attached to the flexible H2A N terminus and thereby not in itself located on the nucleosome core surface.

Second, the specific branched structure of ubiquitin linked to a lysine side chain via an isopeptide bond is not a critical feature, since the genetically-encoded ubiquitin fusions represent linear proteins and also lack the terminal GG motif. Therefore, the specificity must originate from other parts of ubiquitin.

Third, modification-demodification cycles of H2Bub are not required for crosstalk *in vivo*. Steady-state levels of H2Bub are the result of ongoing ubiquitination by Bre1/Rad6 and deubiquitination by Ubp8 and Ubp10 (Schulze et al., 2011). It has been proposed that turnover of histone modifications could be an important determinant of epigenetic regulation (Henry et al., 2003; Scheuermann et al., 2010). However, since our non-cleavable ubiquitins could promote H3K79 and H3K4 methylation, we conclude that H3 methylation can be promoted without H2Bub turnover.

Fourth, Bre1 activity towards non-nucleosomal substrates is not a requirement for the crosstalk, since ubiquitins tethered to the nucleosome confer crosstalk to H3 methylation in the absence of Bre1. It has been suggested that the Bre1/Rad6 ubiquitination machinery, rather than H2BK123ub, pro-

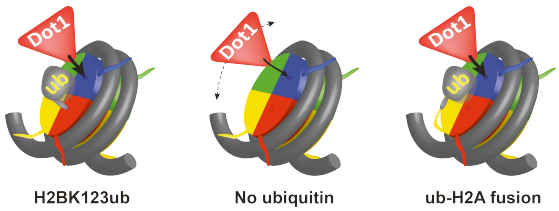

Figure 4.5: Schematic representation of a crash barrier model for the role of H2Bub in promoting histone methylation. Ubiquitin, if in the correct orientation, can interact with the nucleosome and coach Dot1 towards H3K79, thereby increasing Dot1's chances of a productive encounter. See text.

motes maximal crosstalk, potentially by ubiquitinating Swd2 (Thornton et al., 2014; Vitaliano-Prunier et al., 2008). However, this mechanism is still under debate (Soares and Buratowski, 2013). In our strains the presence of ubiquitin on the nucleosome is uncoupled from Bre1 activity. Our finding that tethered ubiquitins can promote H3 methylation in the absence of Bre1 argues against a critical role of the ubiquitination machinery. However, since even the most efficient tethered ubiquitins we engineered did not fully rescue H3K4me3 and H3K79me3, it is still possible that the Bre1-dependent ubiquitination of a non-histone protein has an additional effect.

Fifth, the orientation of the ubiquitin seems to be a critical structural feature. The C terminus of H2B and the N terminus of H2A are at approximately the same distance from H2BK123 (Supplementary Figure 4.3B and C). Yet, ubiquitin tethered to H2AS1 was much more effective in histone crosstalk. One key structural difference is that the ubiquitin on the N terminus of H2A is presented in the same orientation as the native ub on H2BK123 whereas ubiquitin on the C terminus of H2B is in the opposite orientation.

We believe that our *in vivo* results, together with previous *in vitro* findings, are most parsimonious with a model in which ubiquitin can interact with the nucleosome surface and thereby increase the chance of a productive encounter of Dot1 with H3K79 on the nucleosome. This could be achieved by creating a physical road block or crash barrier that coaches Dot1 in the right direction (see Figure 4.5). A similar fold-back mechanism has previously been suggested for ubiquitin on PCNA (Freudenthal et al., 2010). Ubiquitin tethered to the N terminus of H2A, both at S19 and S1, would be able to fold back just like the native H2Bub. The ubiquitins tethered to the C-termini, which are in the opposite orientation, would not be able to do this. The modest crosstalk that is still observed for these tethers may occur through another mechanism, possibly as proposed in the wedge or bridge model.

The finding that ubiquitin moieties at locations other than H2B can promote histone methylation suggests that nucleosome crosstalk could also be affected by other ubiquitination events in the cell. This is consistent with the crosstalk

that has been observed between H2BK34ub and H3 methylation (Wu et al., 2011b), but the site of ubiquitination does not have to be limited to H2B or even the nucleosome core. It will be interesting to determine whether the extensive chromatin ubiquitination during DNA damage response in mammalian cells (Jackson and Durocher, 2013b), especially the ubiquitination at the N terminus of H2A (Mattiroli et al., 2012), influences the methylation of resident or newly-assembled histones during the process of DNA repair. The tethered ubiquitins that we describe here are genetically encoded and amenable to genetic manipulation. Therefore, they will provide opportunities to further delineate the role of ubiquitin in the control of histone methylation and other aspects of chromatin structure and function.

4.5 Experimental procedures

Strains, plasmids and growth conditions. Yeast media and growth conditions, and strains and plasmids are described in the Supplementary Methods.

Immunoblotting and mass spectrometry. Histone methylation and expression was determined by immunoblotting and mass spectrometry as described previously (De Vos et al., 2011). See Supplementary Methods.

***In vitro* methyltransferase assays.** Recombinant 10xHis-Dot1 proteins were incubated with yeast nuclear chromatin templates and analyzed by immunoblot analysis as described previously (Frederiks et al., 2008). See Supplementary Methods.

DNA damage checkpoint activation. Yeast cells were arrested in G1 for two hours, exposed to 100 J/m^2 UV irradiation and recovered for 30 minutes before protein extracts were made, as described previously (Frederiks et al., 2008). See Supplementary Methods.

4.6 Acknowledgments

We thank T. Sixma, F. Mattiroli, I. Stulemeijer, and C. McLean for critical reading of the manuscript, M. Terweij for the initial characterization of the RITE strains, Y. Bollen for advice on protein spacer length calculations, T. Richmond for advice and sharing unpublished observations, L. ONeil for providing the H3K4me1 antibody and L. Janssen for the hUb(K0) plasmids. FvL and HV were supported the Dutch Cancer Society (KWF2009-4511) and the Netherlands Genomics Initiative.

4.7 Author contributions

HV and FvL designed the studies, analyzed the data, and wrote the paper. HV and TvW performed the plasmid and strain constructions, yeast manipulations and methyltransferase assays. ELdG, AFMA and AJRH were responsible for mass spectrometry measurements. DO constructed conditional ub-tag cassettes under supervision of PSS.

4.8 Conflict of interest

The authors declare that they have no conflict of interest.

4.9 Supplementary data

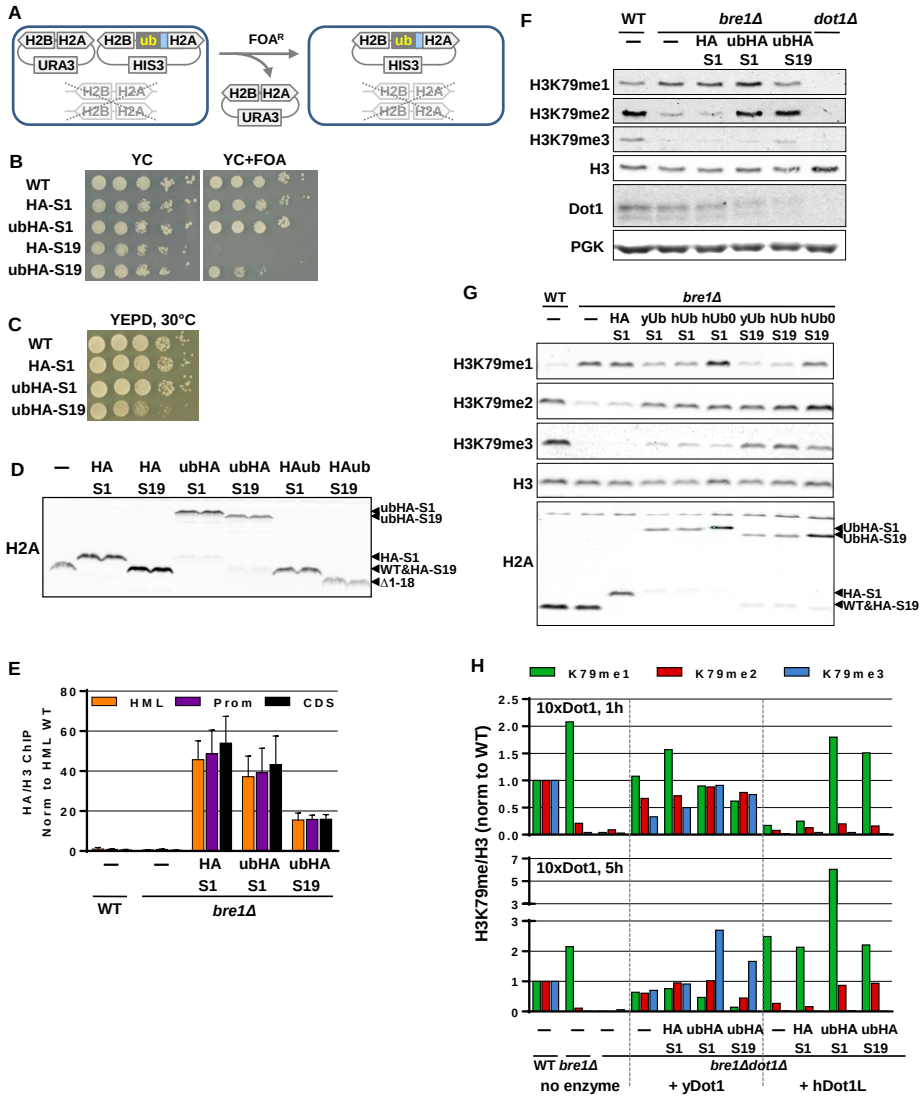

Supplementary Figure 4.1: Effect of ubiquitin tethered to the N-terminus of H2A on H3K79 methylation in vivo and in vitro. A) Plasmid-shuffle assay to replace a *URA3* plasmid encoding wild-type H2A-H2B by a *HIS3* plasmid encoding wild-type or tagged H2A-H2B, in the absence of endogenous H2A-H2B. Cells that lose the wild-type *URA3* plasmid become resistant to 5-FOA. **B)** Plasmid shuffle in *bre1*Δ strains. Serial dilution on media containing 5-FOA to determine the viability of the strains expressing the H2A variants in the absence of wild-type H2A. The lethality of HA-S19-H2A, but not ubHA-S19-H2A,
Continued on next page.

Continuation Supplementary Figure 4.1.
in combination with *bre1*Δ indicates that ubiquitin and the N-terminus of H2A may have a shared function, such as affecting interactions with specific sites on the nucleosome core. This is in agreement with their close proximity on the nucleosome and the finding that the H2A N-terminus promotes H2B ubiquitination (Zheng et al., 2010). **C)** Growth assay after serial dilution on solid media of *bre1*Δ cells expressing wild-type or tagged H2A, obtained as described in Figure 4.2A. **D)** Immunoblot analysis of WT strains (*BRE1+*) expressing wild-type or tagged H2A. Despite deletion of the terminal glycine, which eliminates the canonical GG at the C-terminus of ub that is cleaved by ubiquitin-specific proteases, HAub fusions were cleaved in the cell. **E)** HA ChIP-qPCR of three loci. All values were normalized to H3 and then to wild-type at the *HML* locus. Primer sets against *HML*, the promoter of the *GAL1* gene and the coding sequence of *SPA2* were used. Mean $\pm$ SD of three biological replicates. Note: quantitative differences may be caused by the variable context of the HA epitope. **F)** H3K79 methylation and Dot1 immunoblot analysis of strains analyzed by MS in Figure 4.2C. textbfG) Immunoblot analysis of strains expressing indicated H2A mutants. The effect of yeast ubiquitin, human ubiquitin and human ubiquitin with all lysines mutated to arginines was compared. Note: although the original construct contained the wild-type human Ub sequence, the (independent) KO clones generated by gap-repair and selected in yeast contained a P19A mutation. This site is one of the few that is not conserved from yeast to human; yeast ubiquitin contains an S at this position. **H)** Quantification of immunoblots of two independent *in vitro* methyltransferase assays, as described in Figure 4.2. Experiment of Figure 4.2E was done with 1x Dot1 for 1 hour, for these blots the assay conditions were 10x Dot1 for 1h and 10x Dot1 for 5h, respectively. Signals for each methylation state were normalized to those in WT (e.g. see MS analyses of Figure 4.2 and Figure 4.3). We note that the catalytic domain of hDOT1L seems to be a less efficient trimethylase than yeast Dot1 under these conditions.

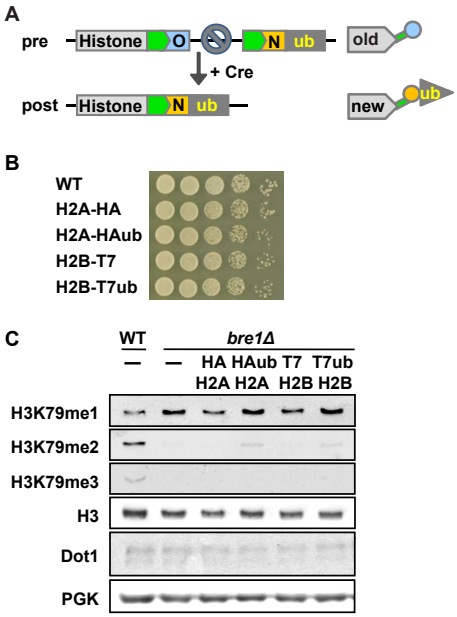

Supplementary Figure 4.2: Effect of ubiquitin tethered to the C-terminus of H2A or H2B on H3K79 methylation *in vivo*. **A)** Outline of recombination-Induced Tag Exchange (RITE) to switch from an old (blue) to a new (orange) tag upon activation of Cre recombinase (Radman-Livaja et al., 2011; Verzijlbergen et al., 2010). RITE-ub cassettes were applied to H2A and H2B in cells lacking Bre1 to switch from an old HA tag to a new T7-tag-ub fusion (ub knock-in), or from an old HA-tag-ub fusion to new T7 tag. **B)** Growth assay after serial dilution on solid media (NKI4530 and derivatives). HA-tag fusions were used for H2A since a short T7 tag without ub was lethal. **C)** Immunoblot analysis of strains described in B and analyzed by MS in Figure 4.3.

A

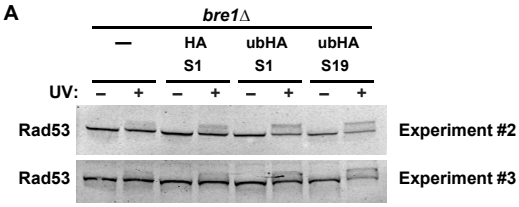

B

>H2B-spacer-LoxP-T7-Ubiquitin
SAKAEKKPASKAPAEKKPAAKKTSTSTDGKKRSKARKETYSSYIYKVLKQT
HPDTGISQKSMSILNSFVNDIFERIATEASKLAAYNKKSTISAREIQTAVRLIL
PGELAKHAVSEGTRAVTKYSSSTQAGGSGGSITSYNVCYTKLSVDMASM
TGGQQMGCTMQIFVKTLTGKTITLEVESSDTIDNVKSKIQDKEGIPPDQQR
LIFAGKQLEDGRTLSDYNIQKESTLHLVLRLRGV

>H2A-spacer-LoxP-HA-Ubiquitin
SGGKGGKAGSAAKASQSRSAKAGLTFPVGRVHRLLRRGNYAQRIGSGAP
VYLTAVLEYLAAEILELAGNAARDNKKTRIIPRHLQLAIRNDDELNKLLGNVT
IAQGGVLPNIHQNLLPKKSAKATKASQELGGSGGSITSYNVCYTKLSGTYP
YDVPDYATSMQIFVKTLTGKTITLEVESSDTIDNVKSKIQDKEGIPPDQQRLI
FAGKQLEDGRTLSDYNIQKESTLHLVLRLRGV

>Ubiquitin-HA-S1-H2A
MQIFVKTLTGKTITLEVESSDTIDNVKSKIQDKEGIPPDQQRLIFAGKQLED
GRTLSDYNIQKESTLHLVLRLRGTSMYPYDVPDYASGSGGKGGKAGSAA
KASQSRSAKAGLTFPVGRVHRLLRRGNYAQRIGSGAPVYLTAVLEYLAAEI
LELAGNAARDNKKTRIIPRHLQLAIRNDDELNKLLGNVTIAQGGVLPNIHQN
LLPKKSAKATKASQEL

>Ubiquitin-HA-S19-H2A
MQIFVKTLTGKTITLEVESSDTIDNVKSKIQDKEGIPPDQQRLIFAGKQLED
GRTLSDYNIQKESTLHLVLRLRGTSMYPYDVPDYASGSAKAGLTFPVGRV
HRLLRRGNYAQRIGSGAPVYLTAVLEYLAAEILELAGNAARDNKKTRIIPRH
LQLAIRNDDELNKLLGNVTIAQGGVLPNIHQNLLPKKSAKATKASQEL

Ubiquitin
SalI VD
BsrGI CT
SpeI TS
BspEI SG
HA (YPYDVPDYA)
T7 (MASMTGGQQMG)
Spacer-LoxP

C

Estimated distance of ubiquitin

From	To	AA	Estimated distance (Å)
H2BK123	H2A-ub	n.a.	opposite side of nucleosome (>100)
H2BK123	H2B-ub	40	34
H2A-S1	ub-HA-S1-H2A	32	31
H2A-S19	ub-HA-S19-H2A	14	21

Supplementary Figure 4.3: Position of the tethered ubiquitins. A) Immunoblot analysis of activation of the central DNA damage checkpoint kinase Rad53 upon exposure of yeast cells arrested in G1/S to 100J m^{-2} UV irradiation. Rad53 is activated by phosphorylation, which leads to a mobility shift. Replicates of Figure 4.4B. **B)** Protein sequences of H2B-T7ub, H2A-HAub, ubHA-S1-H2A, ubHA-S19-H2A (Δ1-18). **C)** Estimated average distance of the tethered ubiquitins to the native H2BK123ub site. We assumed random coils, based on the conformations of similar flexible peptide linkers as determined by FRET sensors (Evers et al., 2006).

Supplementary Table 4.1: Summary of the effects of the tethered ubiquitins on H3 methylation. Summary of crosstalk between tethered ubiquitins and H3K79 and H3K4 methylation. H3K79me scores are based on measurements by MS (including the unmethylated state), H3K4me scores are based on immunoblot analysis.

		WT	bre1Δ				
		H2B K123ub	no ub	H2A-ub	H2B-ub	ub-H2A	ub-H2A Δ1-18
H3K79	me0	+	+++	++	++	+	+
	me1	++	+++	++++	++++	+++	++
	me2	++	+	++	++	+++	+++
	me3	+++	-	-	-	+	++
H3K4	me1	+++	-	-	+	++	+++
	me2	+++	-	-	+	++	+++
	me3	+++	-	-	-	+	++

4.10 Supplementary methods

Yeast strains and plasmids. Yeast strains and plasmids used in this study are listed in Supplementary Table 2 and 3, respectively. Yeast media have been described previously (Van Leeuwen et al., 2002). NKI4602 was derived from a cross between UCC7315 with BY4727 (Brachmann et al., 1998; Gardner et al., 2005). Plasmids swaps were used to generate all derivatives of NKI4602. NKI8001 was derived from BY4733 (Brachmann et al., 1998) by inserting the conditional Cre recombinase from pTW040 (Verzijlbergen et al., 2010) and by deleting *BAR1* using pMPY-ZAP (Schneider et al., 1996). Gene deletions were made by standard gene replacement by homologous recombination. Conditional C-terminal ubiquitin tagging cassettes were made by cloning one ubiquitin-encoding sequence of UBI4 and inserting it into the *Spe*I or *Bsr*GI site of the RITE vector pFvL118 (Verzijlbergen et al., 2010), resulting in pDOP1 and pDOP2, respectively. The C-terminal glycine of ubiquitin was mutated to valine to avoid conjugation of the ub-fusion proteins to ubiquitination substrates. The modified RITE cassettes were amplified and targeted by homologous recombination to the C-terminus of H2A (*HTA1*) and H2B (*HTB1*) in yeast strains lacking the second H2A and H2B locus. Integrated RITE cassettes conferred resistance to Hygromycin. Tag swapping was induced in the absence of Hygromycin by addition of -estradiol, as described previously (De Vos et al., 2011; Verzijlbergen et al., 2010). Plasmid pHV007 was derived from pJH23 by swapping *HIS3* by *URA3* by homologous recombination in yeast. Ubiquitin (*UBI4*) was introduced at the N-terminus of H2A on S1 or S19 on the H2A-H2B shuffle plasmid (pJH23) (Gardner et al., 2005; Hirschhorn et al., 1995) by first introducing an HA-tag flanked by *Spe*I and *Bsp*EI restriction sites by site-directed mutagenesis using overlap-extension PCR (pHV008, pHV009), and then inserting at the *Spe*I or *Bsp*EI site one ubiquitin-encoding sequence of *UBI4* of which the C-terminal glycine of ubiquitin was deleted to avoid cleavage by ubiquitin-specific proteases. hUb and hUbK0 were amplified from Addgene plasmids 11928 (Dantuma et al., 2006) and 11934 (Bergink et al., 2006), respectively, deleting the C-terminal glycine and introducing a 40bp overhang. The amplicons were co-transformed into NKI4606, together with SpeI-digested and Klenow-treated pHV008 or pHV009. Cells that grew out on YC-HIS and had repaired the plasmid using the hUb(K0)-containing amplicon were selected for further analysis and verified by sequencing of the insert.

Immunoblotting. Whole-cell extracts were obtained from approximately $5x10^7$ cells by the glass beads breakage method using 200µL of glass beads and 500µL SUMEB lysis buffer containing 1µM DTT (Frederiks et al., 2008) complemented with PMSF (1mM), benzamidine (5mM), pepstatin (1µg/mL), and leupeptin (1µg/mL). The resulting lysates were separated on 8%, 16% or gradient polyacrylamide gels. For immunoblots, proteins were transferred onto 0 45µm nitrocellulose membranes. Membranes were blocked with 2% Nutrilon

(Nutricia) in PBS. Primary antibody incubations were performed overnight in Tris-buffered saline-Tween (TBST) with 2% Nutrilon. For quantitative immunoblotting, secondary antibody incubations were performed for 45 minutes in TBST with 2% Nutrilon at room temperature using LI-COR Odyssey IRDye 800CW (1:12.000). Immunoblots were subsequently scanned on a LI-COR Odyssey IR Imager (Biosciences) using the 800 channel. Signal intensities were determined using Odyssey LI-COR Image Studio 2.0. H3K79 methylation signals were normalized to H3-C signals. Dot1 signals were normalized to Pgk1 signals. The rabbit polyclonal antibodies against Dot1, H3K79me1, H3K79me2, H3K79me3, and the C-terminus of H3 were described before (De Vos et al., 2011; Frederiks et al., 2008). The H3K4me1 antibody was a gift from Laura ONeil. Commercially available antibodies that were used in this study are H3K4me2 (07-030, Upstate), H3K4me3 (ab8580, Abcam), H3K79me2 (04-835, Millipore), H2B (39238, Active Motif), H2A (39236, Active Motif), and Pgk1 (A-6457, Invitrogen), Rad53 (sc-6749, Santa Cruz).

Mass spectrometry. For mass spectrometry, histones were separated on a 16% SDS-PAGE gel and stained with Coomassie Blue. The band corresponding to histone H3 was excised from the gel and shrunk twice with 100µL acetonitrile. The proteins in the gel band were digested overnight at 37°C with 500ng of Endoproteinase Arg-C (Roche Applied Science) in 85µL (10mM CaCl2, 100mM Tris, pH 7.6) and 10µL activation solution (50mM DTT, 5mM EDTA). The supernatant was collected and vaporized using a Speedvac (New Brunswick Scientific). To measure H3K79 methylation levels, samples were dissolved in 10% formic acid prior to reverse phase nano-flow liquid chromatography on an Agilent 1200 LC system coupled to multiple reaction monitoring mass spectrometry (nLC-MRM) on a TSQ Vantage (Thermo Scientific). Briefly, peptides were loaded on a 20mm x 100µm ID C18 trap column (packed in house ReproSil-Pur C18-AQ, 3µm, (Dr. Maisch GmbH, Ammerbuch, Germany) at 5µL/min solvent A (0 1M acetic acid); followed by an online separation on an analytical column (ReproSil-Pur C18-AQ, 3µm (Dr. Maisch GmbH, Ammerbuch, Germany); 40 cm x 50µm ID, packed in house) in a 30min linear gradient from 10 to 50% solvent B (0 1M acetic acid in 8:2 (v/v) acetonitrile:water) at ˜100nL/min. Peptide ionization was achieved using the Nanospray ion source (Thermo Scientific) and fused silica gold coated emitters (pulled and coated in house) at 1 7kV. The mass spectrometer was configured to select precursor ions at 0.7 FWHM in Q1, fragment peptides at 1.5 mTorr Argon and m/z dependent collision energies (factory default) in Q2, using tuned S-Lens values and an acquisition cycle time of 2 seconds. This resulted in a minimum of 30 milliseconds per transition and peaks spanning at least 11 data points. MRM transitions and parameters were chosen and optimized using a set of 4 quantified and purified synthetic peptides with the sequence EIAQDFK*TDLR (K*: K-me0, -me1, -me2 and -me3). Briefly, doubly and triply charged precursors were fragmented on the TSQ Vantage and their 4 most abundant fragment ions were selected and validated using Skyline software (MacCoss Lab). Label free quantification was achieved by comparing

the area of each methylation state to the sum of the area of all methylation states. As the 4 different peptides have slightly different physicochemical properties and thus might have slightly different ionization efficiencies in the mass spectrometer, final peptide intensities were corrected using a relative response factor to obtain more accurate results. The relative response factor was obtained by measuring the peak areas of the four differently methylated peptides from an equimolar mixture and dividing peptide areas by the area of the unmethylated peptide. Because of technical issues associated with the detection of methylated H3K4 by mass spectrometry, H3K4 methylation was only analyzed by immunoblotting.

***In vitro* methyltransferase assays.** The catalytic domain of hDot1L (1–430) was cloned into pET16b (Novagen) and expressed as a 10xHis fusions in E. coli BL21(DE3)pLysS (Novagen). Recombinant Dot1 proteins were purified using Talon Metal Affinity Resin (ClonTech) as previously described (Frederiks et al., 2008; Van Leeuwen et al., 2002). Yeast nuclear chromatin templates were prepared from frozen pellets of ˜5x10^8 log-phase cells. Cells were broken in 2mL screw cap tubes by bead beating in 300µL (20mM Hepes-KOH pH 7.0, 250mM sucrose, 10mM $MgCl_2$, 0.1% Triton Tx-100 (v/v), 5mM β-mercaptoethanol, 2 5mM spermidine, 0 5mM spermine). After removing the glass beads the lysate was diluted with 1mL lysis buffer, and spun. The chromatin in the pellet was solubilized in chromatin-isolation buffer (20mM Hepes-KOH pH 7.0, 200mM NaCl, 10mM $MgCl_2$, 0.1% Triton Tx-100 (v/v), 10% glycerol (v/v), 5mM β-mercaptoethanol) by sonication (highest setting, 2 cycles of 30" on and 30" off) in a Bioruptor (Diagenode). Following centrifugation (5' 14,000 RPM in a microfuge) the soluble chromatin was transferred to a new tube. *In vitro* methyltransferase reactions were carried out at 30°C for 1h or 5 h in 50µL reactions containing 10mM Tris-HCl, pH 8.0, 320µM SAM, 20µL chromatin template, and 1 or 10µL Dot1 protein (˜0.2–2 and 1–10µg10 g for yDot1 and hDOT1L, respectively). Reactions were terminated by addition of 12µL 5xSDS-PAGE loading buffer and analyzed by immunoblot analysis.

DNA-damage checkpoint activation. Exponentially growing cells (optical density (OD) 0.5) were arrested in G1-S with 5mg/mL α-factor for 2h, spun, resuspended in fresh media containing α-factor and plated on 14-cm Petri dishes. The plates were irradiated with 100J/m^2 UV light of 254nm using a Stratalinker (Stratagene). 30 min after irradiation, trichloroacetic acid protein extracts were prepared. Protein extracts were blotted for Rad53, see Immunoblotting.

ChIP-qPCR. Chromatin immunoprecipitation experiments were performed mostly as described in (Terweij et al., 2013). Fixing was done for 15 minutes and 2mL screw-cap tubes and zirconia/silica beads were used for bead beating. After the first wash with FA, the pellet was resuspended in 450µL FA containing 0.8% SDS to denature the epitopes. This was then sonicated for 10 minutes with 30 sec on-off cycles on high power. Debris was pelleted

for 5 min at 4°C at 20,817 x g and the supernatant was sonicated for another 5 minutes. 1mL FA (no SDS) was added to the combined samples of the two tubes and chromatin was cleared by centrifugation for 5 min at 4°C at 20,817 x g. This chromatin was used in the ChIP directly, without micrococcal nuclease digestion. Extra FA was added to the samples before the ChIP to prevent denaturation of the antibodies. The antibodies used in the ChIP were the same as for immunoblots.

qPCRs were performed with SYBRgreen master mix (Roche) and using the LightCycler 480 II (Roche). qPCR primers are shown in Supplementary Table 4.

Nucleosome structure. The nucleosome core particle (PDB 1ID3) (White et al., 2001) was visualized in Swiss PDB viewer.

Supplementary Table 4.2: Yeast strains used in this study.

Strain	Genotype	Reference
BY4727	MATα lys2Δ0 trp1Δ63 his3Δ200 ura3Δ0 leu2Δ?0 met15Δ0	Brachmann *et al*, 1998
UCC7315	MATa lys2Δ0 trp1Δ63 his3Δ200 ura3Δ0 leu2Δ0 met15Δ0 ade2::hisG ADE2-TEL-VR URA3-TEL-VIIL hta1-htb1Δ::MET15 hta2-htb2Δ::LEU2 pCS1 (pCEN-LYS2-HTA1-HTB1)	Gardner *et al*, 2005
NKI4602	MATa lys2Δ0 trp1Δ63 his3Δ200 ura3Δ0 leu2Δ0 met15Δ?0 hta1-htb1Δ::MET15 hta2-htb2Δ::LEU2 pCS1 (pCEN-LYS2-HTA1-HTB1)	This study
NKI4606	MATa lys2Δ0 trp1Δ63 his3Δ200 ura3Δ0 leu2Δ0 met15Δ0 hta1-htb1Δ::MET15 hta2-htb2Δ::LEU2 pHV007 (pCEN-URA3-HTA1-HTB1)	This study
NKI4614	MATa lys2Δ0 trp1Δ63 his3Δ200 ura3Δ0 leu2Δ0 met15Δ0 hta1-htb1Δ::MET15 hta2-htb2Δ::LEU2 pJH23 (pCEN-HIS3-HTA1-HTB1)	This study
NKI4615	MATa lys2Δ0 trp1Δ63 his3Δ200 ura3Δ0 leu2Δ0 met15Δ0 hta1-htb1Δ::MET15 hta2-htb2Δ::LEU2 pHV008 (pCEN-HIS3-HA-S1-HTA1-HTB1)	This study
NKI4617	MATa lys2Δ0 trp1Δ63 his3Δ200 ura3Δ0 leu2Δ0 met15Δ0 hta1-htb1Δ::MET15 hta2-htb2Δ::LEU2 pHV021 (pCEN-HIS3-ub-HA-S1-HTA1-HTB1)	This study
NKI4616	MATa lys2Δ0 trp1Δ63 his3Δ200 ura3Δ0 leu2Δ0 met15Δ0 hta1-htb1Δ::MET15 hta2-htb2Δ::LEU2 pHV009 (pCEN-HIS3-HA-S19-HTA1(Δ1-18)-HTB1)	This study
NKI4618	MATa lys2Δ0 trp1Δ63 his3Δ200 ura3Δ0 leu2Δ0 met15Δ0 hta1-htb1Δ::MET15 hta2-htb2Δ::LEU2 pHV022 (pCEN-HIS3-ub-HA-S19-HTA1(Δ1-18)-HTB1)	This study
NKI4624	MATa lys2Δ0 trp1Δ63 his3Δ200 ura3Δ0 leu2Δ0 met15Δ0 hta1-htb1Δ::MET15 hta2-htb2Δ::LEU2 bre1Δ::KanMX pHV007 (pCEN-URA3-HTA1-HTB1)	This study
NKI4625	MATa lys2Δ0 trp1Δ63 his3Δ200 ura3Δ0 leu2Δ0 met15Δ0 hta1-htb1Δ::MET15 hta2-htb2Δ::LEU2 bre1Δ::KanMX pJH23 (pCEN-HIS3-HTA1-HTB1)	This study
NKI4626	MATa lys2Δ0 trp1Δ63 his3Δ200 ura3Δ0 leu2Δ0 met15Δ0 hta1-htb1Δ::MET15 hta2-htb2Δ::LEU2 bre1Δ::KanMX pHV008 (pCEN-HIS3-HA-S1-HTA1-HTB1)	This study
NKI4628	MATa lys2Δ0 trp1Δ63 his3Δ200 ura3Δ0 leu2Δ0 met15Δ0 hta1-htb1Δ::MET15 hta2-htb2Δ::LEU2 bre1Δ::KanMX pHV021 (pCEN-HIS3-ub-HA-S1-HTA1-HTB1)	This study
NKI4629	MATa lys2Δ0 trp1Δ63 his3Δ200 ura3Δ0 leu2Δ0 met15Δ0 hta1-htb1Δ::MET15 hta2-htb2Δ::LEU2 bre1Δ::KanMX pHV022 (pCEN-HIS3-ub-HA-S19-HTA1(Δ1-18)-HTB1)	This study
NKI4619	MATa lys2Δ0 trp1Δ63 his3Δ200 ura3Δ0 leu2Δ0 met15Δ0 hta1-htb1Δ::MET15 hta2-htb2Δ::LEU2 pHV024 (pCEN-HIS3-HA-ub-S1-HTA1-HTB1)	This study
NKI4620	MATa lys2Δ0 trp1Δ63 his3Δ200 ura3Δ0 leu2Δ0 met15Δ0 hta1-htb1Δ::MET15 hta2-htb2Δ::LEU2 pHV025 (pCEN-HIS3-HA-ub-S19-HTA1(Δ1-18)-HTB1)	This study
NKI4631	MATa lys2Δ0 trp1Δ63 his3Δ200 ura3Δ0 leu2Δ0 met15Δ0 hta1-htb1Δ::MET15 hta2-htb2Δ::LEU2 bre1Δ::KanMX dot1Δ::NatMX pJH23 (pCEN-HIS3-HTA1-HTB1)	This study
NKI4636	MATa lys2Δ0 trp1Δ63 his3Δ200 ura3Δ0 leu2Δ0 met15Δ0 hta1-htb1Δ::MET15 hta2-htb2Δ::LEU2 bre1Δ::KanMX dot1Δ::NatMX pHV008 (pCEN-HIS3-HA-S1-HTA1-HTB1)	This study
NKI4637	MATa lys2Δ0 trp1Δ63 his3Δ200 ura3Δ0 leu2Δ0 met15Δ0 hta1-htb1Δ::MET15 hta2-htb2Δ::LEU2 bre1Δ::KanMX dot1Δ::NatMX pHV021 (pCEN-HIS3-ub-HA-S1-HTA1-HTB1)	This study
NKI4634	MATa lys2Δ0 trp1Δ63 his3Δ200 ura3Δ0 leu2Δ0 met15Δ0 hta1-htb1Δ::MET15 hta2-htb2Δ::LEU2 bre1Δ::KanMX dot1Δ::NatMX pHV022 (pCEN-HIS3-ub-HA-S19-HTA1(Δ1-18)-HTB1)	This study
BY4733	MATa leu2Δ0 met15Δ0 trp1Δ63 ura3Δ0 his3Δ200	Brachmann *et al*, 1998
NKI8001	MATa leu2Δ0 met15Δ0 trp1Δ63 ura3Δ0 his3Δ200::HIS3-GPD-CRE-EBD78 bar1Δ::HISG	This study
NKI4516	MATa leu2Δ0 met15Δ0 trp1Δ63 ura3Δ0 his3Δ200::HIS3-GPD-CRE-EBD78 bar1Δ::HISG hta2-htb2Δ::MET15	This study
NKI4530	MATa leu2Δ0 met15Δ0 trp1Δ63 ura3Δ0 his3Δ200::HIS3-GPD-CRE-EBD78 bar1Δ::HISG hta2-htb2Δ::MET15 bre1Δ::KanMX	This study
NKI4536	MATa leu2Δ0 met15Δ0 trp1Δ63 ura3Δ0 his3Δ200::HIS3-GPD-CRE-EBD78 bar1Δ::HISG hta2-htb2Δ::MET15 bre1Δ::KanMX hta1Δ::HTA1-LoxP-HA-HphMX-LoxP-T7	This study
NKI4537	MATa leu2Δ0 met15Δ0 trp1Δ63 ura3Δ0 his3Δ200::HIS3-GPD-CRE-EBD78 bar1Δ::HISG hta2-htb2Δ::MET15 bre1Δ::KanMX hta1Δ::HTA1-LoxP-HA-ub-HphMX-LoxP-T7	This study
NKI4522	MATa leu2Δ0 met15Δ0 trp1Δ63 ura3Δ0 his3Δ200::HIS3-GPD-CRE-EBD78 bar1Δ::HISG hta-htb2Δ::MET15 bre1Δ::KanMX htb1Δ::HTB1-LoxP-HA-HphMX-LoxP-T7	This study
NKI4551	MATa leu2Δ0 met15Δ0 trp1Δ63 ura3Δ0 his3Δ200::HIS3-GPD-CRE-EBD78 bar1Δ::HISG hta-htb2Δ::MET15 bre1Δ::KanMX htb1Δ::HTB1-LoxP-HA-HphMX-LoxP-T7ub	This study
NKI4546	MATa leu2Δ0 met15Δ0 trp1Δ63 ura3Δ0 his3Δ200::HIS3-GPD-CRE-EBD78 bar1Δ::HISG hta-htb2Δ::MET15 bre1Δ::KanMX htb1Δ::HTB1-LoxP-T7	This study
NKI4552	MATa leu2Δ0 met15Δ0 trp1Δ63 ura3Δ0 his3Δ200::HIS3-GPD-CRE-EBD78 bar1Δ::HISG hta-htb2Δ::MET15 bre1Δ::KanMX htb1Δ::HTB1-LoxP-T7ub	This study
NKI4545	MATa leu2Δ0 met15Δ0 trp1Δ63 ura3Δ0 his3Δ200::HIS3-GPD-CRE-EBD78 bar1Δ::HISG hta2-htb2Δ::MET15 bre1Δ::KanMX htb1Δ::HTB1-LoxP-HA-HphMX-LoxP-T7	This study
NKI4539	MATa leu2Δ0 met15Δ0 trp1Δ63 ura3Δ0 his3Δ200::HIS3-GPD-CRE-EBD78 bar1Δ::HISG hta2-htb2Δ::MET15 bre1Δ::KanMX htb1Δ::HTB1-LoxP-HA-ub-HphMX-LoxP-T7	This study
NKI4566	MATa leu2Δ0 met15Δ0 trp1Δ63 ura3Δ0 his3Δ200::HIS3-GPD-CRE-EBD78 bar1Δ::HISG hta2-htb2Δ::MET15 bre1Δ::KanMX dot1Δ::NatMX	This study

Supplementary Table 4.3: Plasmids used in this study.

Plasmid	Description	Reference
pHV007	CEN URA3 HTA1 HTB1	This study
pCS1	CEN LYS2 HTA1 HTB1	Gardner *et al*, 2005
pJH23	CEN HIS3 HTA1 HTB1	Hirschhorn *et al*, 1995
pHV008	CEN HIS3 HA-S1-HTA1 HTB1	This study
pHV009	CEN HIS3 HA-S19-HTA1(Δ1-18) HTB1	This study
pHV021	CEN HIS3 ub-HA-S1-HTA1 HTB1	This study
pHV022	CEN HIS3 ub-HA-S19-HTA1(Δ1-18) HTB1	This study
pHV024	CEN HIS3 HA-ub-S1-HTA1 HTB1	This study
pHV025	CEN HIS3 HA-ub-S19-HTA1(Δ1-18) HTB1	This study
pFvL118	spacer-LoxP-HA-HphMX-LoxP-T7	Verzijlbergen *et al*, 2010
pDOP1	spacer-LoxP-HA-Ub-HphMX-LoxP-T7	This study
pDOP2	spacer-LoxP-HA-HphMX-LoxP-T7-Ub	This study
Addgene 11928	GFP-hUb	Dantuma *et al*, 2006
Addgene 11934	GFP-hUbK0	Bergink *et al*, 2006

Supplementary Table 4.4: qPCR primers used in this study.

Primer name	Sequence
HML1down_Qfor	CTTGTCTTCTCTGCTCGCTGAA
HML1down_Qrev	TCCCATATTCCGTGCTGCAT
GAL1_Qfor	TGCTCCGAACAATAAAGATTCTACA
GAL1_Qrev	GGCCAGGTTACTGCCAATTTT
SPA2_High_Qfor	ATCAAGAGAAGAGGGTTCGACAAG
SPA2_High_Qrev	CATCGGCTGCGGTAATGG